



9 **Abstract**

10 Raman, near-infrared and fluorescence spectroscopy were evaluated for determination of collagen  
11 content in ground meat. Two sample sets were used (i.e. ground beef and ground poultry by-  
12 products), and collagen concentrations (measured as hydroxyproline) varied in the ranges 0.1 -  
13 3.3% in the beef samples and 0.4 - 1.5% in the poultry samples. Similar validation results for  
14 hydroxyproline were obtained for NIRS ( $R^2 = 0.82$  and RMSECV = 0.11%) and Raman ( $R^2 =$   
15  $0.81$  and RMSECV = 0.11%) for the poultry samples. For the beef samples, NIRS obtained  
16 slightly less accurate results ( $R^2 = 0.89$ , RMSECV= 0.25%) compared to Raman ( $R^2 = 0.94$ ,  
17 RMSECV= 0.19%), most likely due to less representative sampling. Fluorescence spectroscopy  
18 gave higher prediction errors (RMSECV= 0.50% and 0.13% for beef and poultry, respectively).  
19 This shows that Raman spectroscopy employing a scanning approach for representative sampling  
20 is a potential tool for on-line determination of collagen in meat.

21 **Keywords:** Raman; NIR; fluorescence; collagen; ground meat

22

## 23 **1. Introduction**

24 Collagen is the most abundant mammalian and avian fibrous protein. It is predominantly located  
25 in the skin (or hide), tendons and bones. Different types of collagen are distinguished by their  
26 amino acid composition, with collagen type I-IV being the most abundant. The collagen triple-  
27 helix presents a conformation consisting of glycine-X-Y repeating sequences. The X and Y  
28 positions can accommodate any amino acid in order to form a stable triple-helix. However, when  
29 proline and hydroxyproline are situated in the X and Y positions, respectively, this sequence is  
30 the most stabilizing and most commonly found tripeptide unit present in collagen (Persikov,  
31 Ramshaw, Kirkpatrick, & Brodsky, 2000). In meat, collagen contributes to quality parameters  
32 such as tenderness, texture and sensory properties. In addition, bioprocessing of by-products from  
33 fish and poultry is a growing industry (Aspevik et al., 2017), and collagen is an interesting target  
34 protein for a range of different markets, from food ingredients to cosmetics (Gomez-Guillen,  
35 Gimenez, Lopez-Caballero, & Montero, 2011). Thus, there is a high interest in developing tools  
36 for rapid determination of collagen in meat.

37 The traditional methods for determination of collagen in meat are destructive and time consuming,  
38 usually involving the quantification of hydroxyproline by colorimetric (Kolar, 1990) or  
39 chromatographic (Colgrave, Allingham, & Jones, 2008) methods after complete proteolysis.  
40 Spectroscopic methods, on the other hand, offer fast and non-invasive measurements and can  
41 enable effective quality differentiation and process control (Beganovic, Hawthorne, Bach, &  
42 Huck, 2019). Near-infrared spectroscopy (NIRS) is one of the most frequently used non-  
43 destructive techniques in the meat industries, and NIRS has also been used for determination of  
44 collagen (measured as hydroxyproline) in meat. However, in several studies, unsatisfactory  
45 prediction results have been found for ground beef and ovine meat ( $R^2$  in the range 0.18 - 0.55)  
46 (Alomar, Gallo, Castañeda, & Fuchslocher, 2003; Prieto, Andrés, Giráldez, Mantecón, & Lavín,  
47 2006; Young, Barker, & Frost, 1996). NIRS have been evaluated for the quantification of  
48 hydroxyproline in cured pork sausages and dry cured beef with better results ( $R^2 = 0.77$  and  
49 standard error of prediction of 0.05%) (González-Martín, Bermejo, Hierro, & González, 2009).

50 Recently, other authors used this technique to classify sous-vide loins as a function of time of  
51 cooking and predicted texture-related parameters of the samples (including hydroxyproline) with  
52  $R^2$  of 0.92 and mean absolute scaled error (MASE) of 0.19 (Perez-Palacios, Caballero, González-  
53 Mohíno, Mir-Bel, & Antequera, 2019). In that study, the hydroxyproline concentration range was  
54 larger (2.0 - 4.5%) compared to the previously mentioned studies, which probably improved the  
55 results.

56 The rationale behind using fluorescence spectroscopy for determination of collagen is related to  
57 the fact that several components present in connective tissue, like collagen crosslinks and  
58 components such as pyridinoline and pentosidine, have fluorescing properties (A. J. Bailey, Sims,  
59 Avery, & Halligan, 1995; J. Bailey & Light, 1989). Wold et al. (1999) determined hydroxyproline  
60 in intact slices of beef, with moderate results due to a narrow range of hydroxyproline (0.4 - 0.9%)  
61 (Jens Petter Wold, Kvaal, & Egelanddal, 1999). However, a considerable improvement was  
62 obtained when the range was expanded (0.72 - 7.12%) and samples were homogenized ( $R^2 = 0.94$ ,  
63 RMSECV= 0.37%) (J. P. Wold, Lundby, & Egelanddal, 1999). The potential of fluorescence  
64 was further elucidated for the quantification of hydroxyproline in sausage batters (beef and pork)  
65 with a large variation in myoglobin content (Egelanddal, Dingstad, Tøgersen, Lundby, &  
66 Langsrud, 2005). The concentration of myoglobin largely affects both the intensity and shape of  
67 the fluorescence spectra, and it turned out that prediction errors were reduced slightly when  
68 spectra were normalized by multiplying them by  $a^*$ , i.e. the measured redness of the samples.  
69 The authors found lower prediction errors for fluorescence (0.48%) than for NIRS (0.64%).

70 Raman spectroscopy has the potential to provide detailed chemical information on protein  
71 composition and protein structure (Herrero, 2008). The technique has been employed to obtain  
72 biochemical fingerprints of collagen fibers in native aortic heart valve tissues and to monitor the  
73 increasing damage of collagen fibers (Votteler et al., 2012). Type I and type IV collagens were  
74 characterized by Raman spectroscopy in order to study the relation between aging and cancer  
75 progression (Nguyen et al., 2012). Collagen was also quantified in native and engineered cartilage  
76 tissues with good results ( $R^2 = 0.84$ ) (Bergholt, Albro, & Stevens, 2017). Also, Raman

77 spectroscopy has been used for the characterization of structural changes in collagen, which  
78 allows a more thorough understanding of disease progression (Martinez, Bullock, MacNeil, &  
79 Rehman, 2019). But despite its use in medical diagnostics, only one study reports the  
80 determination of collagen (as hydroxyproline) in meat using Raman spectroscopy (Nian et al.,  
81 2017). The authors obtained good results ( $R^2 = 0.79$ , RMSECV = 0.07%). However, interpretation  
82 of the regression models reveals that some of the main spectral features used for determination of  
83 hydroxyproline was found in a spectral region with no known spectral information related to  
84 proteins (i.e. the spectral region between 1800 and 2800  $\text{cm}^{-1}$ ).

85 Due to the inherent heterogeneity of foods, representative sampling is always a crucial factor in  
86 food analysis. Thus, the main objective of this work was to elucidate the feasibility of Raman  
87 spectroscopy for rapid and non-destructive quantification of collagen in ground meat using a  
88 Raman system equipped with a large volume probe. Two different sample sets were used for this  
89 purpose: 1) samples of ground beef, homogenized in the laboratory and 2) samples of poultry by-  
90 products, industrially ground resulting in less homogeneous samples. A process Raman  
91 instrument was used in scanning mode for all analysis, and to the authors knowledge, this is the  
92 first time that a large volume Raman probe was used for this purpose. For both sample sets, the  
93 performance of Raman spectroscopy was compared with that of NIRS and fluorescence  
94 spectroscopy.

95

## 96 **2. Materials and methods**

### 97 **2.1. Samples**

#### 98 **2.1.1. Beef samples**

99 In order to expand the possible range of collagen and other components in beef samples, a mixture  
100 of different starting materials was used to make 60 different samples. **Different kinds of fats,**  
101 **muscles and tendons** were obtained from a commercial slaughterhouse (Furuseth AS, Dal,  
102 Norway) and food grade collagen powder **usually used for dry sausages, emulsified product etc.**

103 (Collapro Bovine Standard) was supplied from Hulshof Protein Technology, Lichtenvoorde, The  
104 Netherlands. Different amounts of the ingredients were blended to obtain a wide range of  
105 collagen, fat and total protein content in the sample set. **The design of samples can be found in**  
106 **the supplementary material (Table S1).** Samples were ground in a laboratory blender to get  
107 samples as homogeneous as possible. A total of 60 samples (400 g each) were obtained. Before  
108 spectroscopic measurements, the samples were shaped flat with a surface of approximately 160  
109 cm<sup>2</sup> and a thickness of approximately 2 cm.

110

### 111 **2.1.2. Poultry by-products**

112 The poultry by-product sample material was collected from a poultry processing plant (Bioco,  
113 Nortura Hærland, Østfold, Norway). Five by-product fractions were selected, including chicken  
114 skin, and carcasses from both chicken and turkey, before and after mechanical deboning,  
115 respectively. In addition to the pure fractions, the remaining of the 52 samples were prepared by  
116 manually combining 25%, 50% or 75% of the by-product fractions in a range of possible manners  
117 (excluding the 50% -25% -25% versions). **The design of samples can be found in the**  
118 **supplementary material (Table S2).** The samples were ground on-site and immediately measured  
119 with NIRS. 400 g of the sample materials were shaped in the same way as the beef samples and  
120 stored at 4 °C until further analysis by Raman and fluorescence spectroscopy.

### 121 **2.1.3. Pure turkey collagen**

122 A collagen reference sample was extracted from turkey tendons following a literature procedure  
123 (Grønlien et al., 2019). A Raman spectrum was recorded from this sample for comparison with  
124 Raman spectra from more complex beef and poultry samples.

## 125 **2.2. References measurements (Percentage of protein, hydroxyproline and fat)**

126 The references measurements were performed at an external laboratory (ALS laboratory). Two  
127 parallels from each sample were analyzed. Dumas method (Dumas, 1826) was used for total N  
128 and protein content was determined as 6.25\*N-total. An established spectrophotometric method

129 was used for quantifying the hydroxyproline percentage (BS 4401-11:1995, ISO 3496:1994),  
130 generally used as analytical criterion to assess the amount of collagen. In the case of fat content,  
131 an internal method at the ALS laboratory was used based on pulsed nuclear magnetic resonance  
132 (NMR). Samples were dried in an oven to determine the moisture content. After that, samples  
133 were stabilized at 50 °C and resonance of samples were determined. The fat content was  
134 determined automatically by comparing the resonance of the sample with a calibration curve  
135 established using a certified olive oil content.

### 136 **2.3. Spectroscopic measurements**

137 The Raman spectra were collected with a RamanRXN2™ Hybrid system equipped with a non-  
138 contact PhAT-probe (Kaiser Optical Systems, Inc., Ann Arbor, MI, USA). A laser with a 785 nm  
139 excitation wavelength, and a circular spot size of  $D = 6$  mm at a 25 cm working distance was  
140 used. The spectral range was 300-1890  $\text{cm}^{-1}$ . Each spectrum was an average of  $4 \times 20$  sec  
141 accumulations. All measurements were performed by moving the samples manually under the  
142 laser beam, assuring that large parts of the sample surface were probed. The purpose of this  
143 procedure was to obtain representative sampling of the inhomogeneous samples. Each sample  
144 was measured in triplicate and the average spectrum was obtained after fluorescence background  
145 correction.

146 For practical reasons, two different instruments were used for the NIRS measurements. The beef  
147 samples were measured using a FOSS NIRSystems XDS Optiprobe Analyzer™ (FOSS Analytical  
148 A/S, Hillerød, Denmark). Using a fibre-optic probe, the measurements were done in reflectance  
149 mode with a spectral range of 400-2500 nm and a resolution of 0.5 nm. The spectra were  
150 transformed from reflectance to absorbance units ( $A = \log_{10}(1/R)$ ). The probe head was positioned  
151 so that it was in contact with the sample surfaces. Replicate spectra from each sample were  
152 acquired in five different spots ( $D = 1$  cm) and the average spectrum was used for further analysis.

153 In the case of the poultry by-products samples, a Perten DA7440 Process NIR Sensor (Perten  
154 Instruments, a PerkinElmer Company, USA) was used to obtain spectra in reflection mode at a  
155 25 cm working distance. The spectral range was 950-1650 nm with a resolution of 5 nm. The

156 samples were spread out on a board and each spectrum was acquired as an average of 10 seconds  
157 of acquisition while the samples were moved manually under the spectrometer to scan most of  
158 the sample surface. The spectra were transformed from reflectance to absorbance units. Three  
159 replicate spectra were obtained for each sample and a different surface was scanned each time to  
160 obtain a representative sample spectrum. The average spectrum was used for further analysis.

161 The fluorescence emission spectra were measured in front-face mode using a Fluoromax-4  
162 spectrofluorometer (Horiba Scientific, Kyoto, Japan) equipped with a FL-300/FM4-3000  
163 bifurcated fiber-optic probe. The probe head was positioned 5 cm from the sample surface to  
164 create a 4 cm measurement area. The probe and the sample were shielded from ambient light. The  
165 excitation wavelength was set at 340 nm and emission spectra were recorded in the range 360 -  
166 600 nm at every 4 nm. The excitation and emission slit widths were 5 nm. For each sample,  
167 replicate spectra were recorded in five different spots on the sample surface and the average  
168 spectrum was used for further analyses.

169

#### 170 **2.4. Spectral pre-processing and data analysis**

171 The fluorescence background in the Raman spectra was removed from the raw spectra by  
172 applying a commonly used background correction approach based on fitting a polynomial to the  
173 baseline (Lieber & Mahadevan-Jansen, 2003). The procedure was applied to the range 476 - 1890  
174  $\text{cm}^{-1}$ . A polynomial degree of 4 was used. The correction was performed using in-house adapted  
175 automated Matlab scripts (R2007b, The MathWorks, Inc., Natick, MA, USA).

176 NIR and fluorescence spectra were normalized using standard normal variate (SNV) (Barnes,  
177 Dhanoa, & Lister, 1989). For the NIR spectra of the beef samples, a data reduction was performed  
178 so that the spectral range and resolution would be identical to that of the poultry by-products  
179 samples, i.e. a 950-1650 nm range and a 5 nm resolution.

180 Calibration models were based on partial least-squares regression (PLSR) (Martens & Naes,  
181 1989). Full cross-validation was used to determine the number of components to use in the  
182 calibration and to evaluate the performance of the models. The SNV pre-processing and



183 multivariate calibrations were performed using The Unscrambler version 6.11 (CAMO Software  
184 AS, Oslo, Norway).

185

### 186 **3. Results and discussion**

#### 187 **3.1. Sample gross composition**

188 For all samples included in this study (n = 112), collagen (measured as hydroxyproline content),  
189 protein and fat contents were determined as percentage of wet weight. An overview of the gross  
190 composition of the samples is provided in Table 1. The beef samples span a wider range of  
191 hydroxyproline content compared to the poultry by-product samples.

192 Correlation coefficients (Pearson's r) between the different chemical components are also  
193 provided in Table 1. A moderate positive correlation between protein and hydroxyproline content  
194 is seen in both sample sets, which is reasonable since collagen is part of the total protein content.  
195 A weak negative correlation is seen between protein and fat content in the beef samples. For the  
196 poultry by-products, however, a stronger negative correlation between protein and fat is seen.  
197 This is due to the fact that the proportion of chicken skin in the samples, which are high in fat and  
198 low in protein content, is responsible for the main variation of the fat and protein content in the  
199 data set. Finally, extremely weak correlations are seen between hydroxyproline and fat content in  
200 both sample sets.

#### 201 **3.2. Spectral information**

##### 202 **3.2.1. Raman**

203 Baseline-corrected Raman spectra are presented in Figure 1. As expected, the spectra are  
204 dominated by signals originating from fat, with strong Raman bands at 1062, 1129, 1268 (=CH  
205 bending, scissoring), 1300 (C-H bending, stretching), 1442 (C-H bending, scissoring), 1655 (C=C  
206 stretching) and 1742 (RC=OOR, C=O stretching)  $\text{cm}^{-1}$ . Some of these bands are related to  
207 saturated fatty acids or ester groups (1300, 1442 and 1744  $\text{cm}^{-1}$ ) whereas others are related to  
208 unsaturated fatty acids (1655 and 1268  $\text{cm}^{-1}$ ) (Lee et al., 2018). No clear visible trend in the spectra

209 was observed according to the contents of hydroxyproline, which was as expected since  
210 hydroxyproline was low in concentration, and since hydroxyproline is a relatively weak Raman  
211 scatterer compared to fat. In addition, the collagen bands were partly overlapped by the fat bands.  
212 Clear differences between beef and poultry by-products were observed for the bands 960, 970  
213 and 1269  $\text{cm}^{-1}$ , all of which were more pronounced in the poultry by-products. 960  $\text{cm}^{-1}$  is the  
214 phosphate band ( $\nu_1 \text{PO}_4^{3-}$ ), and stems from bone residue (Wubshet, Wold, Böcker, Sanden, &  
215 Afseth, 2019). The bands at 970 and 1269  $\text{cm}^{-1}$  can be assigned to unsaturated fatty acids and the  
216 degree of fatty acid unsaturation (Lee et al., 2018).

### 217 3.2.2. NIR

218 Preprocessed absorption spectra from beef (upper panel) and poultry by-products (lower panel)  
219 samples are shown in Figure 2. For both sample sets, the main bands appeared at 1200 and 1450  
220 nm, where water, protein and fat bands overlap. A clear trend for fat content was observed around  
221 1200 nm in both sets (Figure 2A and 2B) assigned to the second overtone of C-H stretching of  
222 several chemical groups (-CH<sub>2</sub>, -CH<sub>3</sub>, -CH=CH-) (Hourant, Baeten, Morales, Meurens, &  
223 Aparicio, 2000). No spectral variation due to hydroxyproline contents could be detected by visual  
224 inspection of the NIR spectra colored according to hydroxyproline content (Figure 2C and 2D).

### 225 3.2.3. Fluorescence spectra

226 Figure 3 shows the pre-processed fluorescence spectra for beef (upper panel) and poultry by-  
227 products (lower panel) samples. For excitation at 340 nm, collagen has a broad emission band  
228 peaking at about 400 nm (Wagnières, Star, & Wilson, 1998). It is also well known that the  
229 myoglobin in meat reabsorbs the created fluorescence, and valleys therefore appear in the  
230 fluorescence spectra at wavelengths where myoglobin has absorption peaks (Egelanddal et al.,  
231 2005). This explains the valleys at around 410, 548 and 579 nm. The position of the myoglobin  
232 absorption peak at around 410 nm shifts according to exposure to oxygen and might explain the  
233 observed shifts in the corresponding valley in the beef spectra. The reabsorption of myoglobin  
234 makes the fluorescence spectra rather complex, with low intensity for samples with much

235 myoglobin and very strong intensity for samples with little myoglobin. These intensity differences  
236 were removed by pre-processing and are not visible in Figure 3. For the beef samples, no clear  
237 tendency was observed due to differences in fat and hydroxyproline content. There was a slight  
238 shift in the spectra from 450 to 440 nm for those samples with higher hydroxyproline content, but  
239 this can be related to the concentration of myoglobin. Maxima for collagen around 390 nm and  
240 450 nm were reported by Wold et al., 1999 (J. P. Wold et al., 1999), and these can be seen quite  
241 clearly in the spectra from poultry by-products (Figure 3D). Fat, or adipose tissue, has an emission  
242 peak around 475 nm (J. P. Wold et al., 1999), and this can be seen as a shoulder in the region  
243 475 – 525 nm in the spectra from fatty poultry by-products samples (Figure 3B). The origin of  
244 this fluorescence is not certain. The cofactor NADH could be a candidate, but this would fade  
245 over time (Wu, Dahlberg, Gao, Smith, & Bailin, 2019) and introduce instability in the system.  
246 NADH would also be found in other cellular tissues. Lipo-pigments fluoresce in the range 500-  
247 600 nm but are mainly products of lipid oxidation and the presence in fresh meat is therefore less  
248 likely. The very fat poultry samples contained much poultry skin, and skin contains elastin, which  
249 also has a strong fluorescence peaking at 410 nm.

### 250 **3.3. Regression analysis**

251 The descriptive statistics of the different regression models based on Raman spectra are presented  
252 in Table 2. Corresponding “predicted vs. reference”-plots are provided in the supplementary  
253 material. High coefficients of determination ( $R^2$ ) were obtained between measured and estimated  
254 hydroxyproline for both the beef samples and the poultry by-products. Lower prediction errors  
255 (RMSECV) were obtained for the poultry by-products. The comparatively lower  $R^2$  for the  
256 poultry by-products model was ascribed to a narrower range of hydroxyproline concentrations.

257 The regression coefficients for the models are shown in Figure 4A. Ideally, for simple regression  
258 models, coefficients with high values should correspond with spectral bands that carry  
259 information about the target component. In this case, some highlighted coefficients clearly  
260 correspond to Raman bands from collagen (Figure 4B) extracted from turkey. These peaks were  
261 found at 855 (proline ring), 877 (hydroxyproline ring), 922 (proline ring), 936 (C–C stretching

262 vibration of the backbone formed by the glycine-X-Y sequences), 1004 (phenylalanine), 1031  
263 (phenylalanine), 1242 (Amide III) and 1670 (Amide I band)  $\text{cm}^{-1}$ . These peaks have previously  
264 been identified in Raman spectra from collagen type I and type IV (Herrero, 2008; Nguyen et al.,  
265 2012). Furthermore, some negative peaks in the regression coefficients found at 1303, 1438 and  
266  $1652 \text{ cm}^{-1}$  are associated with fatty acid chains. Even though the correlations between  
267 hydroxyproline and fat in these data sets are very weak (as shown in Table 1), the peaks assigned  
268 to fat could turn out negative due to the simple fact that the fat peaks dominate the spectra and  
269 that they are not related to the contents of hydroxyproline. To verify that these Raman bands did  
270 not influence the model, the variables were removed, and new models were obtained ( $R^2 = 0.92$   
271 and  $0.82$ , and  $\text{RMSECV} = 0.20\%$  and  $0.11\%$ , for beef samples and poultry by-products,  
272 respectively). Since similar results were obtained, this indicates that these fat peaks were not  
273 needed to model the collagen content. Table 2 also shows that combining the two data sets into  
274 one regression model was possible, providing good results with similar number of PLSR  
275 components as for the beef samples. Figure 4A also shows that the regression coefficients of the  
276 combined data sets model were comparable to those of the individual models, suggesting a certain  
277 robustness of the Raman approach across different species.

278 Since moderate positive correlations between protein and hydroxyproline content were seen in  
279 both data sets, it was important to assure that the calibrations for collagen did not rely on the total  
280 protein content. One way of studying this is by investigating the correlations between the  
281 predicted values for protein and hydroxyproline contents, respectively (Eskildsen, Næs, Wold,  
282 Afseth, & Engelsen, 2019). Thus, PLSR models for protein were obtained, and the correlation  
283 coefficients between predicted protein and predicted hydroxyproline was calculated ( $r = 0.64$  and  
284  $r = 0.78$  for beef and poultry by-products, respectively). Since these values are close to the  
285 correlations reported in Table 1, we presume that it is possible to predict hydroxyproline  
286 independently of changes in protein content.

287 Results for calibrations based on NIR and fluorescence are presented in Table 2, and the  
288 corresponding regression coefficients are provided in Figure 4. NIRS gave quite similar results

289 for poultry by-products as obtained by Raman spectroscopy. In the case of the beef samples,  
290 higher prediction errors were obtained with NIRS than with Raman spectroscopy and also more  
291 components were needed to obtain a good model. The slightly poorer result for beef could rely  
292 on less representative sampling, since a laboratory system with a fiber-optic probe, with a limited  
293 sampling spot size, was used. NIRS results were comparable to other studies on the determination  
294 of collagen in pork sausages (González-Martín et al., 2009) and pork loins (Perez-Palacios et al.,  
295 2019). The regression coefficients obtained for beef and poultry by-products were quite different  
296 from each other, suggesting that NIRS models for the prediction of collagen content are more  
297 difficult to use across different species compared to Raman spectroscopy models. Due to the  
298 broad NIR bands in the regression coefficients, it was also difficult to make any conclusive  
299 interpretations. The correlation coefficients obtained between predicted protein and predicted  
300 hydroxyproline from NIRS models were  $r = 0.62$  and  $r = 0.78$  for beef and poultry by-products,  
301 respectively. As in the case of Raman, it is thus reasonable to assume that it is possible to predict  
302 hydroxyproline content independently of variations in protein contents.

303 In the case of fluorescence, the results for beef were not as good as previous work on ground beef  
304 and sausage batter, where prediction errors of 0.37% and 0.48%, respectively, were obtained  
305 (Egelandsdal et al., 2005; J. P. Wold et al., 1999). A difficulty in this study was the large color  
306 difference within the beef samples, spanning from red meat to almost white tissue consisting of  
307 mainly fat and connective tissue. As pointed out above, this color variation results in complex  
308 spectra largely affected by myoglobin in both shape and intensity, and the close relation to the  
309 collagen content is lost. This was partly confirmed when five beef samples, white colored and  
310 with very high fat contents were omitted from the data set and the RMSECV was reduced to  
311 0.39%.

312 The fluorescence results for the poultry samples were better and not that far from the results for  
313 NIRS and Raman. Although these samples were very heterogeneous, the color variations were  
314 not as pronounced as in the beef samples. The fat contents in these samples were also lower than  
315 in the beef, making them less complex. A disadvantage with the fluorescence measurement of the

316 poultry samples compared to Raman and NIR was that a rather limited part of the samples was  
317 measured, i.e. only five small regions. This could result in less representative measurements and  
318 a reduced match with the reference values. The regression coefficients were different between the  
319 two sample sets (Figure 4D) due to different spectral properties. Therefore, it did not make sense  
320 to make a combined model. Due to the complexity of the spectra and some uncertainty with  
321 regards to the present fluorophores, it is difficult to interpret the shape of the regression vectors.  
322 Weaker correlation was observed between predicted protein and predicted hydroxyproline (i.e.  $r$   
323 = 0.19 and  $r = 0.68$  for beef and poultry by-products, respectively). As in the case of Raman and  
324 NIRS, it is thus possible to predict hydroxyproline content independently of variations in protein  
325 contents. However, it is important to note that protein models obtained with fluorescence had  
326 much higher RMSECV compared to Raman and NIRS in the first place.

327 The samples of the present study were made to span the range of collagen contents, resulting in a  
328 slightly wider range of collagen than is normally encountered in industrial samples. However, the  
329 results clearly provide relevant knowledge on which spectroscopic methods that are feasible for  
330 collagen determination in foods. Due to rather small sample sets, all regression models were  
331 validated using full cross-validation, which is normally regarded as a rather optimistic validation  
332 approach. All regression models were cross validated with different validation segment sizes in  
333 order to test robustness, and similar results were obtained for all regression models (not shown),  
334 showing that relevant conclusions can be drawn based on the presented results.

335 Fluorescence spectroscopy provided the poorest regression results of the three techniques in the  
336 study. This can partly be attributed to the color variations seen in the sample sets. For Raman and  
337 NIRS, similar regression results were obtained, with Raman providing slightly better results for  
338 the beef samples. It is interesting to note that Raman spectroscopy is the only of the three  
339 techniques that can provide direct information on hydroxyproline, however, the Raman regression  
340 coefficients also show that other protein-related bands are important in the regression models.  
341 This could anyway contribute to explain why Raman seems to be better than NIRS for providing  
342 generic regression models for collagen contents across different species. Finally, based on the

343 present results, state-of-the-art representative sampling approaches such as large volume probes  
344 seem to enable quantitative Raman analysis of heterogenous food samples. This should encourage  
345 the future industrial use of Raman spectroscopy for food analysis.

#### 346 **4. Conclusions**

347 This study demonstrates the potential of Raman, NIRS and fluorescence spectroscopy for rapid  
348 and non-destructive determination of collagen in different types of ground meat. Fluorescence  
349 spectroscopy is a very sensitive method, but this study shows that the signals are easily distorted  
350 by reabsorption by pigments in varying concentrations. These distortions are not easy to correct  
351 for and make the method less robust and accurate for determination of collagen. NIR spectroscopy  
352 performs well, however, the obtained data suggest that NIR models of collagen are more difficult  
353 to use across different species. The regression models for Raman spectroscopy were good with  
354 low prediction errors, and the models were easy to interpret, clearly highlighting spectral bands  
355 associated with collagen. This shows that the scanning approach presently used for covering a  
356 larger part of the sample makes Raman spectroscopy a potential tool for on-line determination of  
357 collagen in meat.

#### 358 **Conflict of interest**

359 The authors declare that there is no conflict of interest.

#### 360 **Acknowledgement**

361 This work was partially funded by the Norwegian Research Council through the projects  
362 Innovative and Flexible Food Processing Technology in Norway, iProcess (No. 255596/E59) and  
363 Novel cascade technology for optimal utilization of animal and marine by-products, Notably (No.  
364 280709/E50); and by the Norwegian Agricultural Food Research Foundation through the projects  
365 FoodSMaCK - Spectroscopy, Modelling & Consumer Knowledge (No. 262308/F40) and Smart  
366 sensor and optimization systems for future food biorefineries, SmartBio (No. 282466/E50).

367 Olga Monago Maraña thanks to the Fundación Ramón Areces for a postdoctoral fellowship for  
368 studies abroad in the field of Life and Matter Sciences (XXXI edition of grants, 2019/2020) to  
369 support her postdoctoral studies at Nofima, Ås, Norway.



370 **References**

- 371 Alomar, D., Gallo, C., Castañeda, M., & Fuchslocher, R. (2003). Chemical and discriminant  
372 analysis of bovine meat by near infrared reflectance spectroscopy (NIRS). *Meat Science*,  
373 63(4), 441–450.
- 374 Aspevik, T., Oterhals, Å., Rønning, S. B., Altintzoglou, T., Wubshet, S. G., Gildberg, A., ...  
375 Lindberg, D. (2017). Valorization of Proteins from Co- and By-Products from the Fish and  
376 Meat Industry. *Topics in Current Chemistry*, 375(3).
- 377 Bailey, A. J., Sims, T. J., Avery, N. C., & Halligan, E. P. (1995). Non-enzymic glycation of  
378 fibrous collagen: Reaction produces of glucose and ribose. *Biochemical Journal*, 305, 385–  
379 390.
- 380 Bailey, J., & Light, N. D. (1989). *Connective tissue in meat and meat products*. London: Elsevier  
381 Science Publishers.
- 382 Barnes, R. J., Dhanoa, M. S., & Lister, S. J. (1989). Standard normal variate transformation and  
383 de-trending of near-infrared diffuse reflectance spectra. *Applied Spectroscopy*, 43(5), 772–  
384 777. <https://doi.org/10.1366/0003702894202201>
- 385 Beganovic, A., Hawthorne, L. M., Bach, K., & Huck, C. W. (2019). Critical review on the  
386 utilization of handheld and portable Raman spectrometry in meat science. *Foods*, 8(2).
- 387 Bergholt, M. S., Albro, M. B., & Stevens, M. M. (2017). Online quantitative monitoring of live  
388 cell engineered cartilage growth using diffuse fiber-optic Raman spectroscopy.  
389 *Biomaterials*, 140, 128–137.
- 390 Colgrave, M. L., Allingham, P. G., & Jones, A. (2008). Hydroxyproline quantification for the  
391 estimation of collagen in tissue using multiple reaction monitoring mass spectrometry.  
392 *Journal of Chromatography A*, 1212, 150–153.
- 393 Dumas, J. B. (1826). Memorie sur quelques points de la Theorie atomistique. *Annales of Chimie*,  
394 33, 342.
- 395 Egelanddal, B., Dingstad, G., Tøgersen, G., Lundby, F., & Langsrud, Ø. (2005).  
396 Autofluorescence quantifies collagen in sausage batters with a large variation in myoglobin  
397 content. *Meat Science*, 69(1), 35–46.
- 398 Eskildsen, C., Næs, T., Wold, J., Afseth, N., & Engelsen, S. (2019). Visualizing indirect  
399 correlations when predicting fatty acid composition from near infrared spectroscopy  
400 measurements. *Proceedings of the 18th International Conference on Near Infrared*  
401 *Spectroscopy*, 39–44.
- 402 Gomez-Guillen, M. C., Gimenez, B., Lopez-Caballero, M. E., & Montero, M. P. (2011).

403 Functional and bioactive properties of collagen and gelatin from alternative sources: A  
404 review. *Food Hydrocolloids*, 25(8), 1813–1827.

405 González-Martín, M. I., Bermejo, C. F., Hierro, J. M. H., & González, C. I. S. (2009).  
406 Determination of hydroxyproline in cured pork sausages and dry cured beef products by  
407 NIRS technology employing a fibre-optic probe. *Food Control*, 20(8), 752–755.

408 Grønlien, K. G., Pedersen, M. E., Sanden, K. W., Høst, V., Karlsen, J., & Tønnesen, H. H. (2019).  
409 Collagen from Turkey (*Meleagris gallopavo*) tendon: A promising sustainable biomaterial  
410 for pharmaceutical use. *Sustainable Chemistry and Pharmacy*, 13.

411 Herrero, A. M. (2008). Raman spectroscopy for monitoring protein structure in muscle food  
412 systems. *Critical Reviews in Food Science and Nutrition*, 48(6), 512–523.

413 Hourant, P., Baeten, V., Morales, M. T., Meurens, M., & Aparicio, R. (2000). Oil and fat  
414 classification by selected bands of near-infrared spectroscopy. *Applied Spectroscopy*, 54,  
415 1168–1174.

416 Kolar, K. (1990). Colorimetric determination of hydroxyproline as measure of collagen content  
417 in meat and meat products: NMKL collaborative study. *Journal of the Association of*  
418 *Official Analytical Chemists*, 73(1), 54–57.

419 Lee, J. Y., Park, J. H., Mun, H., Shim, W. B., Lim, S. H., & Kim, M. G. (2018). Quantitative  
420 analysis of lard in animal fat mixture using visible Raman spectroscopy. *Food Chemistry*,  
421 254(August 2017), 109–114.

422 Lieber, C. A., & Mahadevan-Jansen, A. (2003). Automated method for subtraction of  
423 fluorescence from biological Raman spectra. *Applied Spectroscopy*, 57(11), 1363–1367.

424 Martens, H., & Naes, T. (1989). *Multivariate Calibration*. New York: Wiley.

425 Martinez, M. G., Bullock, A. J., MacNeil, S., & Rehman, I. U. (2019). Characterisation of  
426 structural changes in collagen with Raman spectroscopy. *Applied Spectroscopy Reviews*,  
427 54(6), 509–542.

428 Nguyen, T. T., Gobinet, C., Feru, J., Brassart-Pasco, S., Manfait, M., & Piot, O. (2012).  
429 Characterization of type I and IV collagens by Raman microspectroscopy: Identification of  
430 spectral markers of the dermo-epidermal junction. *Spectroscopy: An International Journal*,  
431 25, 421–427.

432 Nian, Y., Zhao, M., O'Donnell, C. P., Downey, G., Kerry, J. P., & Allen, P. (2017). Assessment  
433 of physico-chemical traits related to eating quality of young dairy bull beef at different  
434 ageing times using Raman spectroscopy and chemometrics. *Food Research International*,  
435 99, 778–789.

- 436 Perez-Palacios, T., Caballero, D., González-Mohíno, A., Mir-Bel, J., & Antequera, T. (2019).  
437 Near Infrared Reflectance spectroscopy to analyse texture related characteristics of sous  
438 vide pork loin. *Journal of Food Engineering*, 263(February), 417–423.
- 439 Persikov, A. V., Ramshaw, J. A. M., Kirkpatrick, A., & Brodsky, B. (2000). Amino acid  
440 propensities for the collagen triple-helix. *Biochemistry*, 39(48), 14960–14967.
- 441 Prieto, N., Andrés, S., Giráldez, F. J., Mantecón, A. R., & Lavín, P. (2006). Potential use of near  
442 infrared reflectance spectroscopy (NIRS) for the estimation of chemical composition of  
443 oxen meat samples. *Meat Science*, 74(3), 487–496.
- 444 Votteler, M., Carvajal Berrio, D. A., Pudlas, M., Walles, H., Stock, U. A., & Schenke-Layland,  
445 K. (2012). Raman spectroscopy for the non-contact and non-destructive monitoring of  
446 collagen damage within tissues. *Journal of Biophotonics*, 5(1), 47–56.
- 447 Wagnières, G. A., Star, W. M., & Wilson, B. C. (1998). In Vivo Fluorescence Spectroscopy and  
448 Imaging for Oncological Applications. *Photochemistry and Photobiology*, 68, 603–632.
- 449 Wold, J. P., Lundby, F., & Egelanddal, B. (1999). Quantification of connective tissue  
450 (hydroxyproline) in ground beef by autofluorescence spectroscopy. *Journal of Food  
451 Science*, 64(3), 377–383.
- 452 Wold, Jens Petter, Kvaal, K., & Egelanddal, B. (1999). Quantification of intramuscular fat  
453 content in beef by combining autofluorescence spectra and autofluorescence images.  
454 *Applied Spectroscopy*, 53(4), 448–456.
- 455 Wu, B., Dahlberg, K., Gao, X., Smith, J., & Bailin, J. (2019). A rapid method based on  
456 fluorescence spectroscopy for meat spoilage detection. In F. Jain, C. Broadbridge, M.  
457 Gherasimova, & G. Tang (Eds.), *High performance logic circuits for high-speed electronic  
458 systems*. Singapore: World Scientific.
- 459 Wubshet, S. G., Wold, J. P., Böcker, U., Sanden, K. W., & Afseth, N. K. (2019). Raman  
460 spectroscopy for quantification of residual calcium and total ash in mechanically deboned  
461 chicken meat. *Food Control*, 95(June 2018), 267–273.
- 462 Young, O. A., Barker, G. J., & Frost, D. A. (1996). Determination of collagen solubility and  
463 concentration in meat by near infrared spectroscopy. *Journal of Muscle Foods*, 7, 377–387.
- 464

**Table 1.** Composition of samples and correlation coefficients (Pearson's r) among the chemical parameters in ground meat and poultry by-products.

<b>Beef samples</b>					
<b>Parameter (%, w/w)</b>	<b>Min. value</b>	<b>Mean value</b>	<b>Max. value</b>	<b>Correlation coefficients (r)</b>	
<b>Protein</b>	6	22	44	<b>Fat - protein</b>	-0.55
<b>Fat</b>	1.1	19	72	<b>Hydroxyproline - protein</b>	0.65
<b>Hydroxyproline</b>	0.1	0.9	3.3	<b>Hydroxyproline- fat</b>	0.26
<b>Poultry by-products samples</b>					
<b>Parameter (%, w/w)</b>	<b>Min. value</b>	<b>Mean value</b>	<b>Max. value</b>	<b>Correlation coefficients (r)</b>	
<b>Protein</b>	9	16	25	<b>Fat - protein</b>	-0.82
<b>Fat</b>	10	21	42	<b>Hydroxyproline - protein</b>	0.72
<b>Hydroxyproline</b>	0.4	0.7	1.5	<b>Hydroxyproline - fat</b>	-0.36

The correlations were all significant ( $p < 0.05$ )

**Table 2.** Summary of PLSR models obtained for predicting hydroxyproline in ground meat and poultry by-products.

<b>Raman</b>			
	<b>N° comp.</b>	<b>R<sup>2</sup> (CV)</b>	<b>RMSECV (%)</b>
<b>Beef samples</b>	4	0.94	0.19
<b>Poultry by-products</b>	3	0.81	0.11
<b>Combined samples</b>	4	0.91	0.17
<b>NIRS</b>			
	<b>N° comp.</b>	<b>R<sup>2</sup> (CV)</b>	<b>RMSECV (%)</b>
<b>Beef samples</b>	6	0.89	0.25
<b>Poultry by-products</b>	4	0.82	0.11
<b>Fluorescence</b>			
	<b>N° comp.</b>	<b>R<sup>2</sup> (CV)</b>	<b>RMSECV (%)</b>
<b>Beef samples</b>	3	0.57	0.50
<b>Poultry by-products</b>	4	0.74	0.13

466

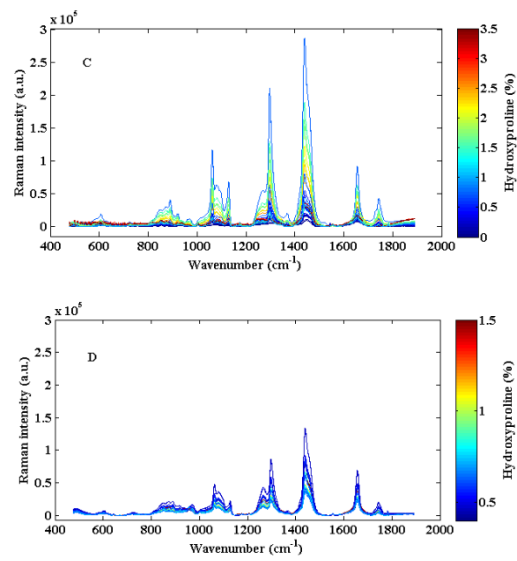
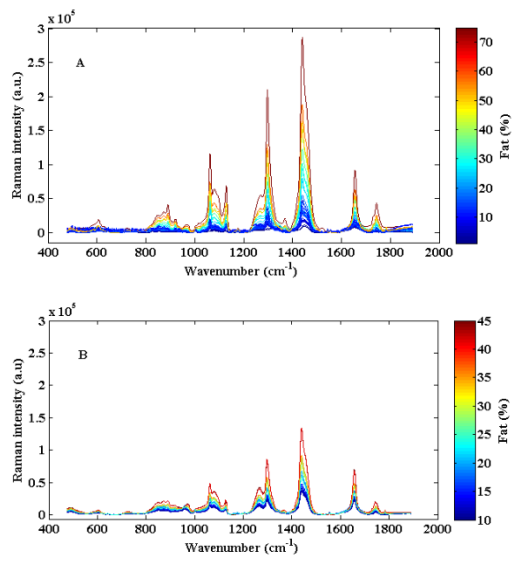
467 **Figure captions**

468 **Figure 1.** Baseline-corrected Raman spectra for beef samples (upper panel) and poultry by-  
469 products (lower panel). The spectra are colored according to percentage of fat (left panel (A, B))  
470 and percentage of hydroxyproline (right panel (C, D)).

471 **Figure 2.** Normalized NIR spectra of beef samples (upper panel) and poultry by-products (lower  
472 panel). The spectra are colored according to percentage of fat (left panel (A, B)) and percentage  
473 of hydroxyproline (right panel (C, D)).

474 **Figure 3.** Normalized fluorescence spectra of beef (upper panel) and poultry by-products (lower  
475 panel). The spectra are colored according to percentage of fat (left panel (A, B)) and percentage  
476 of hydroxyproline (right panel (C, D)).

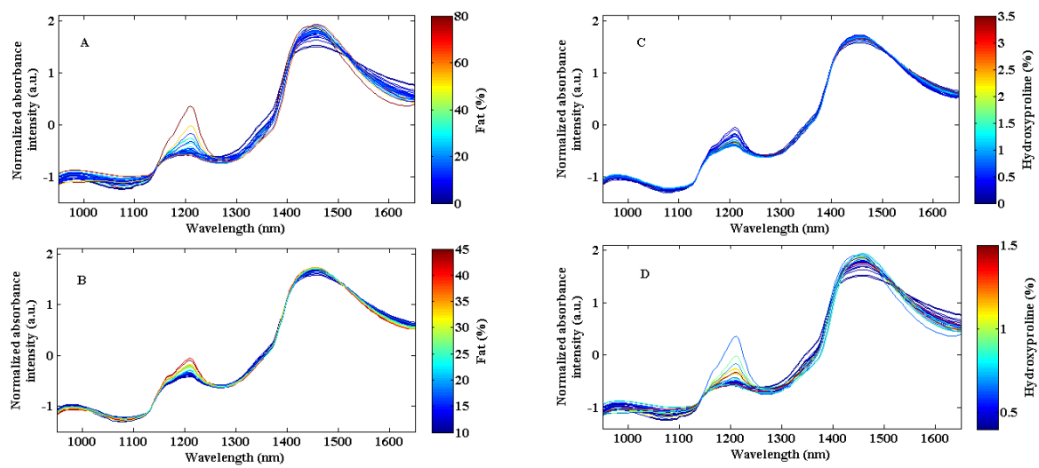
477 **Figure 4.** Regression coefficients for the different models obtained: Raman spectroscopy (A),  
478 NIRS (C) and fluorescence (D). Raman spectrum obtained from collagen extracted from turkey  
479 tendons (B).



480

481 **Figure 1.**

482

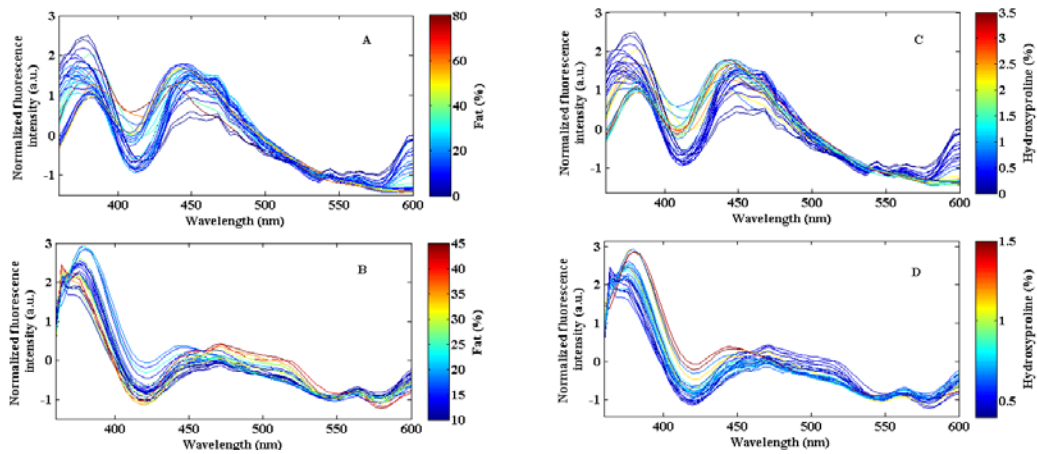


483

484 **Figure 2**

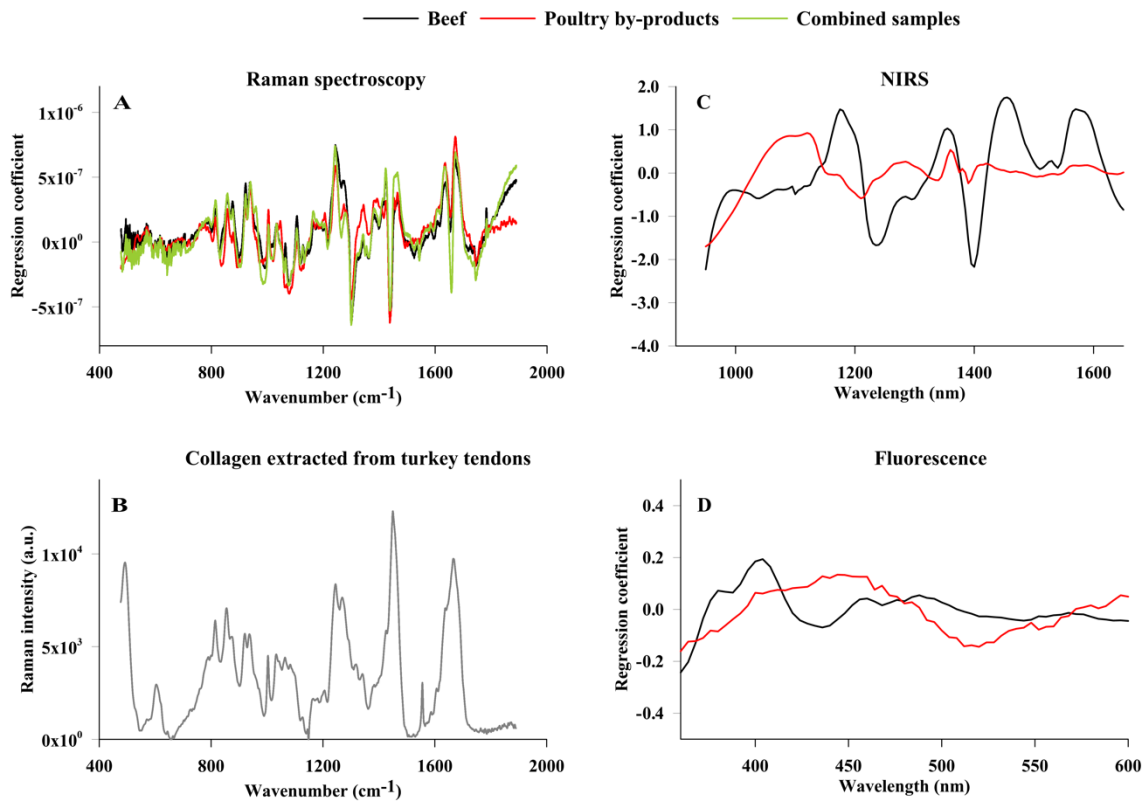


485



486

487 **Figure 3**



489

490

491 **Figure 4.**

492

493